

# Novel in-situ X-ray diffraction measurement of ferroelectric superlattice properties during growth<sup>a)</sup>

Benjamin Bein,<sup>1, b)</sup> Hsiang-Chun Hsing,<sup>1</sup> Sara J Callori,<sup>1, c)</sup> John Sinsheimer,<sup>1, d)</sup> and Matthew Dawber<sup>1, e)</sup>  
*Dept of Physics and Astronomy Stony Brook University, Stony Brook, NY 11794-3800 USA*

Ferroelectric domains, surface termination, average lattice parameter and bilayer thickness were monitored by in-situ x-ray diffraction during the growth of BaTiO<sub>3</sub>/SrTiO<sub>3</sub> (BTO/STO) superlattices by off-axis RF magnetron sputtering. A new x-ray diffraction technique was employed which makes effective use of the custom growth chamber, pilatus detector and synchrotron radiation available at beamline X21, NSLS, BNL. The technique allows for scan times substantially faster than the growth of a single layer of material, allowing continuous monitoring of multiple structural parameters as the film grows. The effect of electric boundary conditions was investigated by growing the same superlattice alternatively on STO substrates and 20nm SRO thin films grown on STO substrates. The growth rate was calibrated using X-ray reflectivity like in<sup>2</sup>.

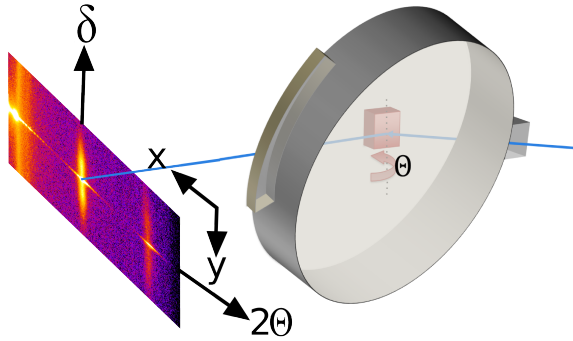


FIG. 1. The figure shows a schematic of the experimental setup and the diffractometer angles. The detector is represented by a snapshot of the data together with the detector coordinate system.

To increase the scan speed to be faster than the growth of one single unit cell layer of material a new scanning technique was employed. The angular integration mode from SPEC called powder mode is used to integrate over the rocking curve of a single crystal. This allows to integrate the exposure of the detector while the  $\theta$  angle is rocked. An example of the taken data is shown in Fig.

2. One can see one single image taken during the experiment and labels of the observed features. These can be assembled into continuous *movies* which allow the observation of the evolution of diffraction features during the growth.

Area scans can be split into two main line scans. The first scan is along the  $q_z$  direction which is a horizontal line in Fig. 2. A plot along this line together with a fit to the data and basic superlattice X-ray diffraction analyzes is shown in Fig. 3. Fitting for superlattice X-ray diffraction is described in<sup>3</sup>. From the fit one can determine surface termination, average lattice parameter  $\bar{c}$  and bilayer thickness. Fig. 4 shows a plot of  $\bar{c}$  against the total superlattice thickness. One can see that all superlattices show a larger tetragonality than one would expect from the known elastic constants for BTO and STO if the samples are paraelectric. This could be explained if the sample is ferroelectric with a out-of-plane component. Furthermore  $\bar{c}$  is larger for the sample grown on a SRO bottom electrode which would suggest a larger polarization of the superlattice grown on a SRO bottom electrode.

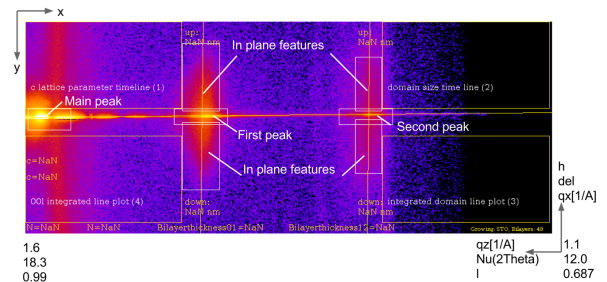


FIG. 2. One single detector image is shown with explanations of the main features one can observe in each scan.

The second line scan is along the  $q_x$  direction which is vertical in Fig 2. The most interesting line for  $q_x$  is in the region where one can observe diffuse scattering. This diffuse scattering is a sign of periodic in-plane features. For ferroelectrics one possible explanation would be stripe domains. This diffuse scattering is shown in Fig. 5, as a vertical cut through the first superlattice peak. The shown data was rescaled to be able to compare the shape of the diffuse scattering for the early stage(7 bilayers) and the end stage(25 bilayers). The rescaling was done by dividing the data by the peak diffuse scattering intensity.

This shows that diffuse scattering gets more intense while the superlattice grows but the average domain size does not change with the square root of the total super-

<sup>a)</sup>This work was supported by NSF DMR1055413

<sup>b)</sup>benjamin.bein@stonybrook.edu

<sup>c)</sup>Now at: Bragg Institute, ANSTO, New Illawarra Road, Lucas Heights NSW 2234, Australia.

<sup>d)</sup>Now at: Brookhaven National Laboratory, Upton, New York 11973-5000, USA.

<sup>e)</sup>matthew.dawber@stonybrook.edu

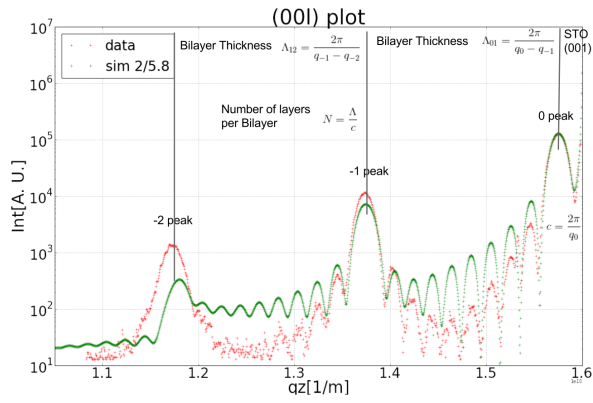


FIG. 3. The figure shows a CTR along (0,0,1) and basic superlattice X-ray diffraction analysis. Furthermore a fit to the superlattice is shown. The fit is used to determine the superlattice characteristics.

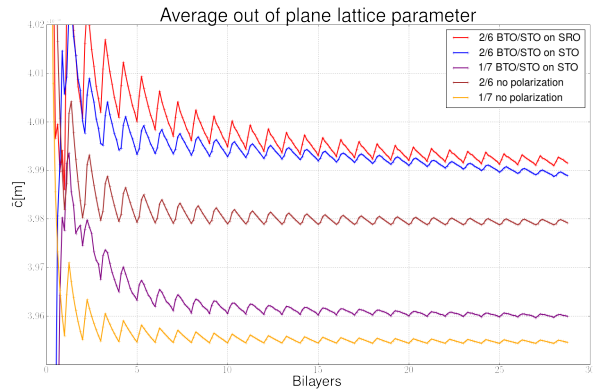


FIG. 4. This plot shows the average out of plane lattice parameter  $\bar{c}$  of the superlattice. The blue curve is  $\bar{c}$  for a 2/6 BTO/STO grown on STO and the red curve is the same superlattice grown on a SRO electrode. The sample grown on SRO has a larger  $\bar{c}$  which suggests a larger polarization. The brown curve would be the expected  $\bar{c}$  for a 2/6 BTO/STO superlattice without any polarization. The purple curve shows  $\bar{c}$  for a 1/7 BTO/STO superlattice grown on STO and the yellow curve is the expected  $\bar{c}$  for the same superlattice without any polarization.

lattice thickness. This suggests that the polarization in the sample is not homogeneously polarized in the out of plane direction. This could be due to closure domains, which are predicted for ultrathin BTO/SRO capacitors<sup>1</sup>. One can write and read domains on the sample using Piezo force microscopy (PFM) which suggests that there is still some cross talk between the different BTO layers. This means that the samples have most likely a mixed state between closure and stripe domains where the out of plane polarization in the STO is smaller than in BTO. Fig. 6 shows a schematic of the mixed domain state. A similar behavior was found for PTO/STO superlattices with only 3 or 4 unit cell layers of PTO per bilayer<sup>4</sup>.

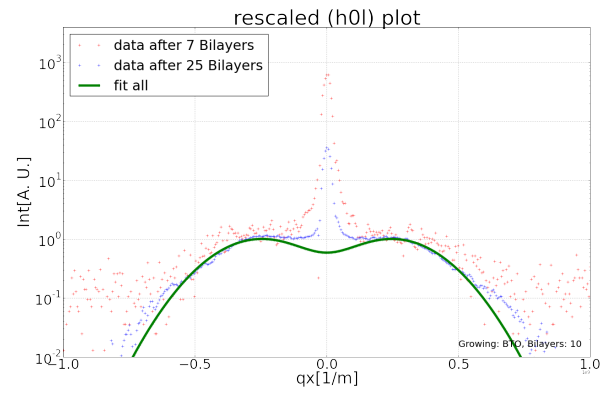


FIG. 5. In the figure one can see a cut along the h direction through the first superlattice peak for two different superlattice thicknesses. The data was rescaled using the domain peak intensity to show that only the absolute intensity of the diffuse scattering changes with time but the distribution does not change. This means that the domain size does not change with thickness.

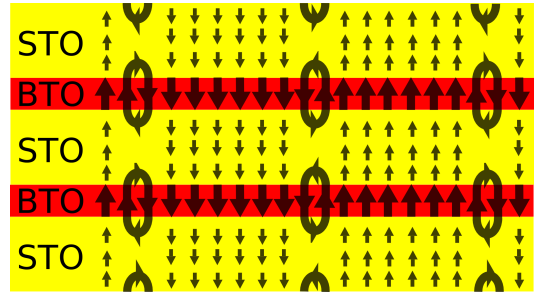


FIG. 6. schematic of ferroelectric domains inside the BTO/STO superlattices.

Besides the fundamental knowledge gained from these studies, being able to monitor the structural parameters of a growing ferroelectric superlattice at this level of detail provides numerous insights which can guide the growth of higher quality ferroelectric superlattices in general.

<sup>1</sup>Pablo Aguado-Puente and Javier Junquera. Ferromagneticlike closure domains in ferroelectric ultrathin films: First-principles simulations. *PHYSICAL REVIEW LETTERS*, 100(17), MAY 2 2008.

<sup>2</sup>Priya V. Chinta, Sara J. Callori, Matthew Dawber, Almamun Ashrafi, and Randall L. Headrick. Transition from laminar to three-dimensional growth mode in pulsed laser deposited BiFeO<sub>3</sub> film on (001) SrTiO<sub>3</sub>. *APPLIED PHYSICS LETTERS*, 101(20), NOV 12 2012.

<sup>3</sup>EE FULLERTON, IK SCHULLER, H VANDERSTRAETEN, and Y BRUYNSEAEDE. STRUCTURAL REFINEMENT OF SUPERLATTICES FROM X-RAY-DIFFRACTION. *PHYSICAL REVIEW B*, 45(16):9292–9310, APR 15 1992.

<sup>4</sup>P. Zubko, N. Jecklin, A. Torres-Pardo, P. Aguado-Puente, A. Gloter, C. Lichtensteiger, J. Junquera, O. Stephan, and J. M. Triscone. Electrostatic Coupling and Local Structural Distortions at Interfaces in Ferroelectric/Paraelectric Superlattices. *NANO LETTERS*, 12(6):2846–2851, JUN 2012.